FRACTURE OF FIBER-REINFORCED BEAMS DUE TO IMPACT LOADING

C. H. Yew, et al

Texas University at Austin

Prepared for:

Ballistic Research Laboratories

March 1975

UNCLASSIFIED

SECURITY CLASSIFICATION OF THIS PAGE (When Data Entered)

REPORT DOCUMENTATION PAGE

READ INSTRUCTIONS BEFORE COMPLETING FORM

1. REPORT NUMBER: BRL Contract Report No. 212
2. GOVT ACCESSION NO.:
3. RECIPIENT'S CATALOG NUMBER: AD-A008 078

4. TITLE (and Subtitle): Fracture of Fiber-Reinforced Beams Due to Impact Loading

5. TYPE OF REPORT & PERIOD COVERED: Final

6. PERFORMING ORG. REPORT NUMBER:

7. AUTHOR(s): C. H. Yew, B. K. Benedict

8. CONTRACT OR GRANT NUMBER(s): DAAD05-73-C-0024

9. PERFORMING ORGANIZATION NAME AND ADDRESS: University of Texas at Austin, Austin, TX 78712

10. PROGRAM ELEMENT, PROJECT, TASK AREA & WORK UNIT NUMBERS: 1T061102A33E

11. CONTROLLING OFFICE NAME AND ADDRESS: US Army Ballistic Research Laboratories, Aberdeen Proving Ground, MD 21005

12. REPORT DATE: MARCH 1975

13. NUMBER OF PAGES: ~~38~~ 26

14. MONITORING AGENCY NAME & ADDRESS (if different from Controlling Office):

15. SECURITY CLASS. (of this report): UNCLASSIFIED

15a. DECLASSIFICATION/DOWNGRADING SCHEDULE:

16. DISTRIBUTION STATEMENT (of this Report)

Approved for public release; distribution unlimited.

17. DISTRIBUTION STATEMENT (of the abstract entered in Block 20, if different from Report)

18. SUPPLEMENTARY NOTES

19. KEY WORDS (Continue on reverse side if necessary and identify by block number)

Solid mechanics impact
Composites
Dynamic fracture
Beams

20. ABSTRACT (Continue on reverse side if necessary and identify by block number)

Experimental studies were made on the dynamic failure of graphite/epoxy fiber reinforced beams of three different angle ply laminates. The cantilevered beam specimens were impacted with tip velocities ranging from 1 ft/sec to 20 ft/sec. Various aspects of the failure of the different types of beams were noted.

DD FORM 1 JAN 73 1473 EDITION OF 1 NOV 65 IS OBSOLETE

UNCLASSIFIED

SECURITY CLASSIFICATION OF THIS PAGE (When Data Entered)

Destroy this report when it is no longer needed.
Do not return it to the originator.

Secondary distribution of this report by originating or sponsoring activity is prohibited.

Additional copies of this report may be obtained from the National Technical Information Service, U.S. Department of Commerce, Springfield, Virginia 22151.

The findings in this report are not to be construed as an official Department of the Army position, unless so designated by other authorized documents.

The use of trade names or manufacturers' names in this report does not constitute indorsement of any commercial product.

TABLE OF CONTENTS

LIST OF ILLUSTRATIONS

I. INTRODUCTION

Due to their high strength, lightweight and potential in many applications, fiber reinforced composite materials have been under intensive investigation for many years. Research in the area of dynamic material properties of composites can, in general, be divided into two areas. The first concerns the propagation of non-destructive pulses or waves in such materials. In these studies, the integrity of the material is preserved. Neither degradation nor fracture are produced in the test specimens during the dynamic loadings. Attenuation and dispersion of waves in the material are the main interest. Literature in this area is abundant. We cite here only a publication of the recent symposium on the dynamics of composite materials [1]*. The second area of research efforts concerns the failure of the composite specimen as a result of dynamic loading. This subject is difficult since, in the authors' opinion, continuum fracture mechanics, until developed far beyond its present state, cannot be, in general, successfully applied to the failure of fiber reinforced composites. This is particularly true when the material is subjected to dynamic loading. Achenback, Herrman, and Ziegler [2] investigated the one-dimensional case of wave propagation normal to the interface of a laminate. They found that fracture between laminae could be caused by impedance mismatching between the laminations. Using plate impact, deRosset [3, 4] has made some detailed studies on the failure of boron-epoxy composites resulting from a plane impact loading. deRosset observed two different modes of failure in the specimen. Debonding between the fibers and matrix, and cracks along the scrim cloth between the layers of fibers were found in the specimen after the test. deRosset attributes the first type of failure to the initial passage of the compressive wave and the second type of failure to the reflected tensile wave. Experimental investigations of the failure mechanisms of glass fiber reinforced epoxy specimens undergoing high rates of tensile loading were made by Armenakas and Sciammarella [5, 6]. They found that the main contribution to the failure of the specimen comes from the breakage of the reinforcing fibers. The number of fiber breaks at high rates of straining is larger than at low rates of straining. Comparing the results obtained by deRosset with that by Armenakas, it is interesting to note that different types of failure were caused by different types of loading. In deRosset's work where the specimens were under plane loading conditions, failure of the specimens was caused mainly be the separation of the reinforcing fibers from the matrix and by the cracks along the layer of fibers; while in Armenakas' work where the specimens were under tensile loading, the breakage of fibers was the main cause of failure of the specimen.

*Numbers in brackets designate to the references at the end of the report.

The strain rate sensitivity of fiber reinforced composites was also reported by Lifshitz [7] and by Schultz and Tsai [8]. All of these studies on dynamic failure have been made on composites with extremely simple configurations (unidirectional reinforcement). The fracture mechanism of more practically valuable angle-ply fiber reinforced laminates is expected to be far more complicated.

Considerable efforts [9], [10], [11], both analytical and experimental, have been made in an attempt for better understanding of the failure mechanism of the composite when it is under a static loading. Some satisfactory theories have been developed for the explanation of the failure of certain types of composites when a fiber reinforced material is subjected to static loading. Nevertheless, when the material is subjected to a dynamic laoding, its failure phenomena are expected to be different from those observed under static loading conditions. The purpose of this investigation is to make an experimental study on the failure of a fiber reinforced material when it is subjected to dynamic loading. A cantilevered beam with its free tip moving with a constant velocity is chosen for this purpose. The tip velocity in this experiment ranges from 1 ft/sec to 20 ft/sec. The reasons for choosing this relatively low deformation velocity are twofold: 1) at high velocity deformation, the specimen suffers a total failure; it often obscures the fine failure mechanism of the specimen, and 2) at high velocity deformation, failure often occurs at the impact region or near the clamped region. Using a cantilevered beam with a relatively low tip velocity avoids this complication. It will become clear in the following section that in the present arrangement, the inertia effects or wave motions of the beam can still be neglected, but the rate effect on the failure of specimen material reveals itself clearly.

II. SPECIMENS AND EXPERIMENTAL ARRANGEMENT

Specimens used in this investigation were Courtauld's 2256 epoxy resin reinforced by HTS graphite as fabricated by the Structural Research Department of the Southwest Research Institute. Beams with three different fibrous configurations were tested. The fiber directions of the three configurations can be described as (0°/90°/90°/0°/90°/90°/0°/90°/90°/0°), (+ 45°/-45°/-45°/+45°/+45°/-45°/-45°/+45°/+45°/-45°/-45°/+45°), and (0°/+45°/-45°/90°/-45°/+45°/0°/0°/+45°/-45°/90°/-45°/+45°/0°). The shorthand notations for these are $(0/90)_{3S}$, $(\pm 45)_{3S}$ and $(0/\pm 45/90/\mp 45/0)_S$ respectively. The 8" x 0.75" beam specimens were cut from the fabricated 12" x 12" panel with a special cutter. Details on fabrication and quality control of the specimens are described in a report by Grimes [12, 13] and they will not be repeated here. It should be mentioned that the properties and failure mechanism of this type of composite under static loading are well documented in these reports.

In order to avoid the effect of the clamp [14, 15], the clamped end of the specimen was wrapped with a 2" wide adhesive tape to a thickness of approximately 1/8". This has proved to be a satisfactory arrangement. All specimen failures occurred outside the clamped region. Grimes [14] has shown that the effect of the clamp on the failure of specimens always reveals itself by cracks initiated from the inside or at the edge of the clamp.

The tape wrapped specimens were then clamped firmly at the base of an impact machine as shown in Figure 1. It is a standard Charpy impact machine with its damping mechanism and standard impact head removed. A Statham type ASOITC-8-350 accelerometer with sensitivity $\pm$ 8 g was attached to the head of the pendulum to monitor its motion. The pendulum was first lifted and then released from a certain height. As the pendulum swung downward, it first passed through two thin aluminum strips placed in front of the specimen for the impact velocity measurement. The signal from the second strip was also used to trigger the oscilloscope which monitors the acceleration- and strain-time relations as the beam specimen is being deformed. A strain gage of effective area 1/4" x 1/4" (SR 4 FAE-25S-1356) was glued on the tensile surface of the specimen at a distance 1/2" from the clamp for measuring the strain. An oscilloscope record is shown in Figure 2. The upper trace is the strain-time relation as the beam deforms. The failure of the beam is signified by a sudden drop of the strain. The lower trace depicts acceleration of the pendulum as it deforms the specimen. At higher impact velocity, the acceleration-time curve is essentially a horizontal straight line. This indicates a constant velocity deformation of the beam. Figure 3 shows the sketch of deformation of beam during impact. The maximum beam tip displacement was 3.75 in. After the pendulum passed the specimen, it was stopped manually to avoid reverse swinging and second loading on the specimen.

Static tests of the beam specimen were performed with approximately the same arrangement. The beam tip movement was controlled manually. The applied force was measured by a load cell. The force-time and strain-time curves were recorded with a strip chart recorder.

III. RESULTS AND OBSERVATIONS

Beams with three different fibrous configuration $[0/90]_{3S}$, $[\pm 45]_{3S}$, $[0/\pm 45/90/\mp 45/0]_S$ were tested with impact velocities ranging from 1 ft/sec to 20 ft/sec. At each velocity, the test was repeated at least once to ensure consistency of the results. The same test was also performed on aluminum beams for comparison. From the results obtained in those tests, the following observations are made:

A) $[0/90]_{3S}$ specimen: A typical strain-time record of such a specimen is shown in Figure 2. The strain varies almost linearly with time until failure of the specimen occurs, which is signified by a sudden drop of the strain. It should be understood, however, that the strain indicated here is not the failure strain of the specimen since failure did not occur at the location of the strain gage. The sudden drop of strain merely indicates the failure of specimen. Since the beam thickness and length ratio is small (less than 0.02) and the end deflection is not large ($\delta_{max} \leq 3.75$ in), it seems justifiable that the deflection of the specimen beam can be described with reasonable accuracy by the elementary beam theory. The failure strain ε_f can then be interpreted from the measured strain ε_m through relation

$$\varepsilon_f = \varepsilon_m \left(1 + \frac{d}{L}\right) \tag{1}$$

where L is the position of the strain gage measured from the free tip of the specimen; and d is the distance from the center of the strain gage to the position where failure occurs.

Since the specimen is black, it is difficult to photograph its failure pattern. A sketch of failure pattern of this type of specimen is presented in Figure 4. It is obvious that delamination occurs between the 0° and the 90° layers. Also, the outer 0° ply and the next two 90° plys break neatly at a position 1/4" above the clamp. It is difficult to deduce from the strain-time and acceleration-time records which of the failure modes occurs first since the strain gage at the present position is not sensitive to the shear deformation between layers. It has been shown [16] that a delaminated beam will have a lower stiffness than a perfectly laminated beam. Thus if delamination indeed occurs prior to the tensile failure of 0° lamination, it should be indicated by a sudden change of slope in the acceleration-time curve. Close examination of the acceleration-time curve appears to indicate that delamination occurs after the tensile failure of the 0° laminate. Furthermore, the magnitude of shear force is constant along the length of the specimen beam in the present test arrangement; thus if delamination were indeed caused by the shear force, it would occur at a point where the shear force has discontinuity, i.e., near the tip portion of the beam. Examining the beam after impact revealed the delamination initiated at the breaking position of the fiber near the clamp and propagated towards the tip of the beam and no delamination was observed near beam tip region.

The specimen tested at low rate of deformation (approximately 2,000 μ in/in) failed at a strain of 10,300 μ in/in due to fiber breakage, and no delamination between layers was noted. This further supports the previous observation on delamination of layers occuring after initial failure of the 0° layers in the impact test. Since the

pendulum head was still in contact with the specimen after the initial failure of 0° layers, delamination was probably caused by the tearing action of the pendulum head.

For comparison purposes, a strain-time curve is shown in Figure 5. A dimensionless plot of the curves in Figure 5 is shown in Figure 6. It is interesting to note that all data points from different impact velocities fell almost into a straight line. Since the maximum beam tip displacement is 3.75" and v equals approximately the beam tip velocity, the beam tip should be separated with the impact pendulum at dimensionless time 1. In Figure 6, the drop of strain occurs at dimensionless time 0.8. The beam thus fails during the process of deformation. Using equation (1), the failure strain of the beams was found to vary from 8,500 to 11,450 μ in/in. Unfortunately, no definite relationship between the failure strain and the impact velocity can be established due to scattering of data.

B) $[\pm 45]_{3S}$ specimen. A typical oscilloscope record of this group of specimens is shown in Figure 7. A continuous strain-time record indicates no measurable failure of specimens in this test. The wavy horizontal portion of strain-time record indicates that the tip of the specimen beam is still in contact with the bottom portion of the pendulum. (This does not affect the interpretation of results, but it is not desirable).

No visible delamination or fracture of these laminates was noted in all the specimens tested. The beam specimen showed however a slight permanent curvature after the test which indicated that plastic deformation of the beam had occured as a result of impact. Figure 8 is a photograph of a specimen beam with an aluminum beam (8" x 0.75" x 1/8") tested with approximately the same impact velocity. The curvature change of aluminum beam is large and localized. This formation of a yield hinge reflects the typical failure pattern of an aluminum beam - a failure due to bending moment. In order to obtain a better understanding of the deformation pattern of the specimen, a free body diagram (Figure 9) of a beam element is helpful. It is clear that the reinforcing fibers are orientted in the direction of pure shear ($\pm$ 45°), thus offering no major reinforcing effect. The specimen beam is expected to behave similarly to a beam made only of the epoxy matrix material which is shown to be non-linear and highly rate dependent.

A dimensionless plot of strain-time records of all the test results is shown in Figure 10. The non-linear behavior of the specimen material is clear when it is compared with test records of aluminum beams.

C) $[0/\pm 45/90/\mp 45/0]_S$ specimen. A typical oscilloscopic record of this specimen is shown in Figure 11. Similar to the $[0/90]_{3S}$ specimen, the failure of specimen is signified by a sudden drop of the

strain-time record. The failure pattern of this specimen, which is sketched in Figure 12, is far more complicated than the $[0/90]_{3S}$ specimen. It reveals a multiple fracture and delamination between layers. A dimensionless plot of all the strain-time records is plotted in Figure 13. When this figure is compared with Figure 5, one can see that failure occurs much sooner and at nearly the same strain level compared to the $[0/90]_{3S}$ specimens.

IV. CONCLUSIONS AND RECOMMENDATIONS

The present experiment has revealed some detailed information on the failure mechanisms of three types of fiber reinforced beams under dynamic bending conditions. Fiber breakages seem to be the dominant factor on the failure of the $[0/90]_{3S}$ specimens. Although shear forces were indeed produced during the loading and the specimen delaminated after test, we attribute this delamination to the tearing action of the pendulum head after the breakage of the fiber rather than to the shear forces. The $[\pm 45]_{3S}$ specimen did not fail physically in the present test arrangement. Neither fracture nor delamination was observed, only a slight permanent curvature change on the beam specimen after the test. As has been explained in the previous section, the fibers in this configuration are not subjected to tensile stress, and thus no breakages of fibers occurred during the test, and the specimen retained its integrity after loading.

Based on the findings of this experiment, the following research is recommended:

A) Carry out the impact test with a higher impact velocity on beams with simple fiber geometry. Detailed information on failure mechanisms of beams with fiber geometry $[\pm 45]$ and $[0/90]$ but with different ply arrangement would provide further insight into the problem and confirmation to the present results.

B) Since the matrix material (epoxy) is an extremely rate sensitive material and the fiber (graphite) is a less rate sensitive material, a test of this fiber reinforced composite at different temperature levels would reveal some detailed information on the interaction between the reinforcing fiber and its surrounding matrix.

C) We propose to develop a theoretical prediction of failure pattern of composite beams with complicated fiber geometry (such as $[0/\pm 45/90 \mp 45/0]_S$ specimen) based on the failure mechanism of beams with simple fiber geometry.

ACKNOWLEDGEMENT

The authors wish to express their appreciation to Dr. J. A. Zukas for his helpful comments and suggestions in preparation of this report.

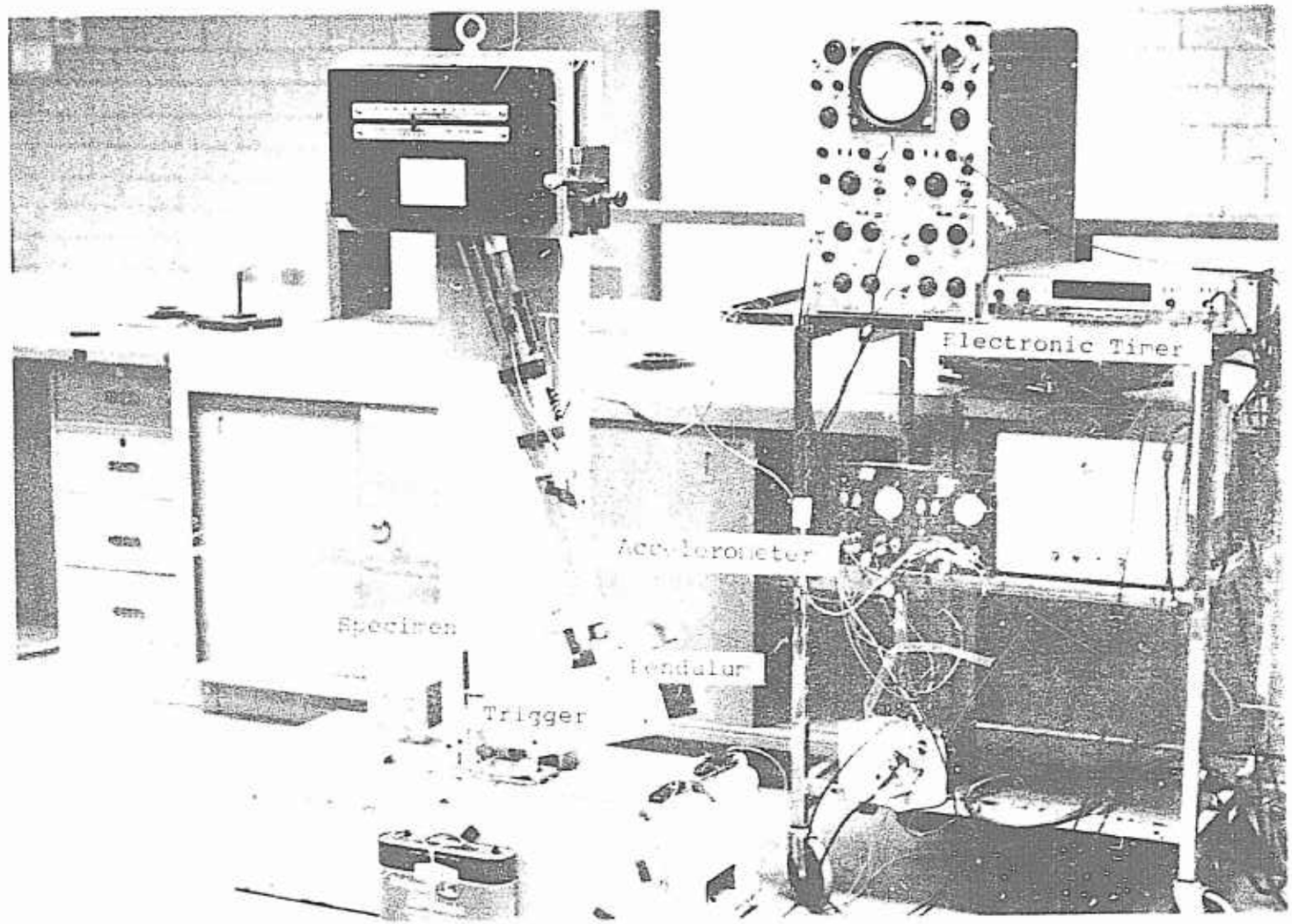

Figure 1. Experimental Configuration

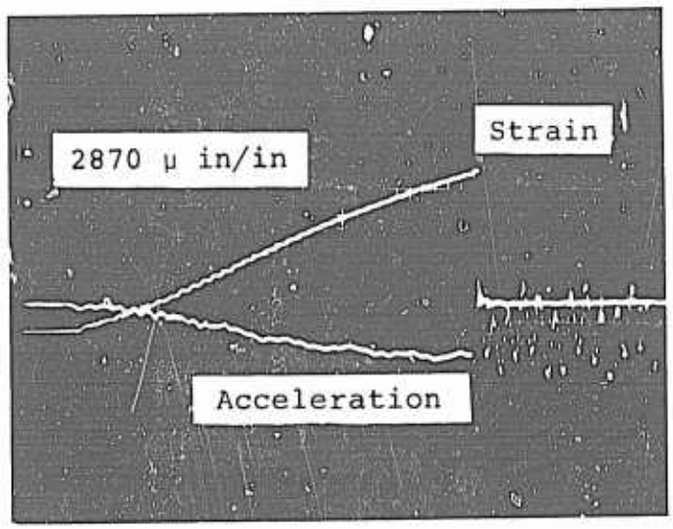

Time = 10 msec/div
Impact velocity = 3.5 ft/sec

Figure 2. Typical Oscilloscope Record, $[0/90]_{3S}$

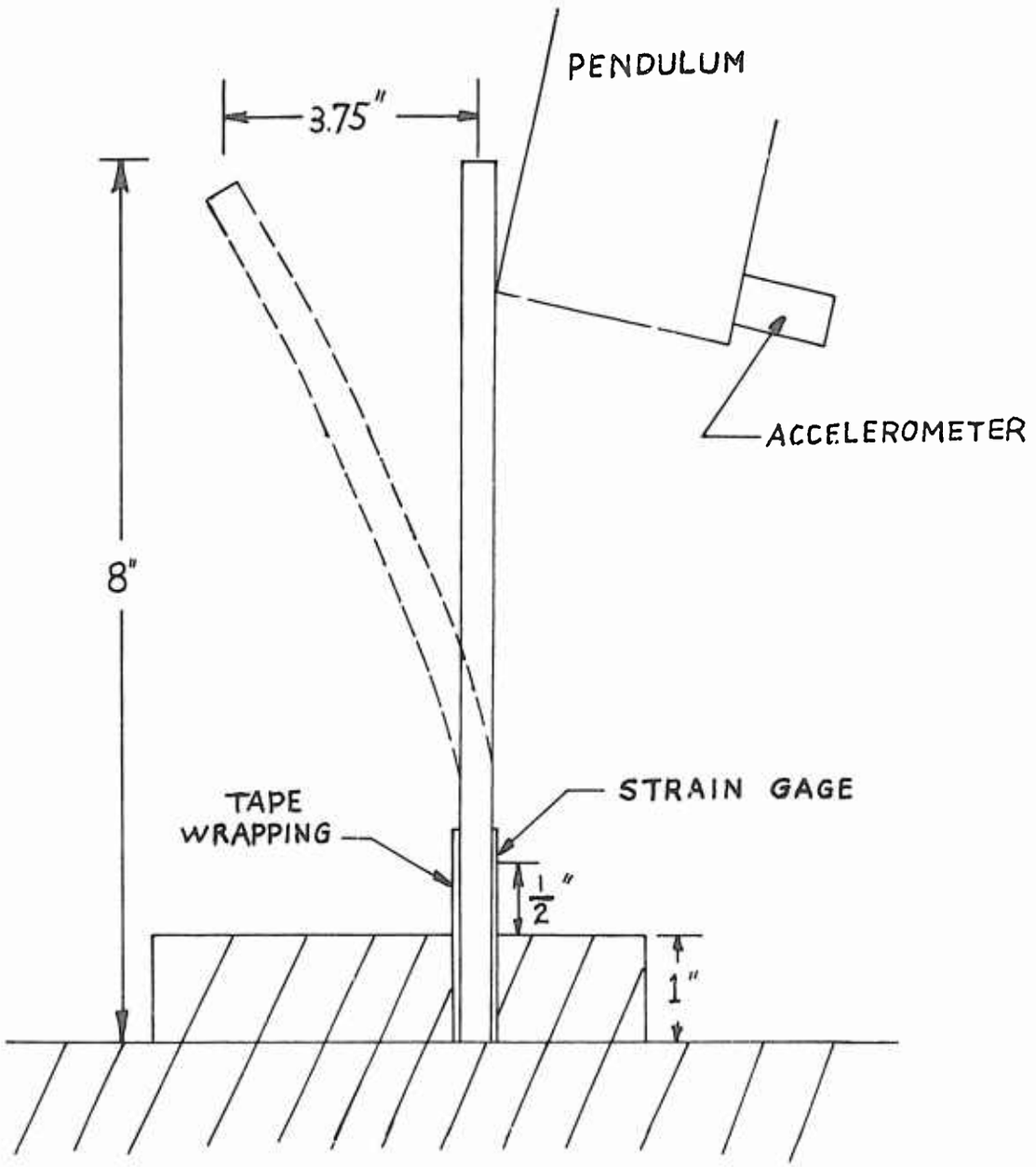

Figure 3. Beam Impact Configuration

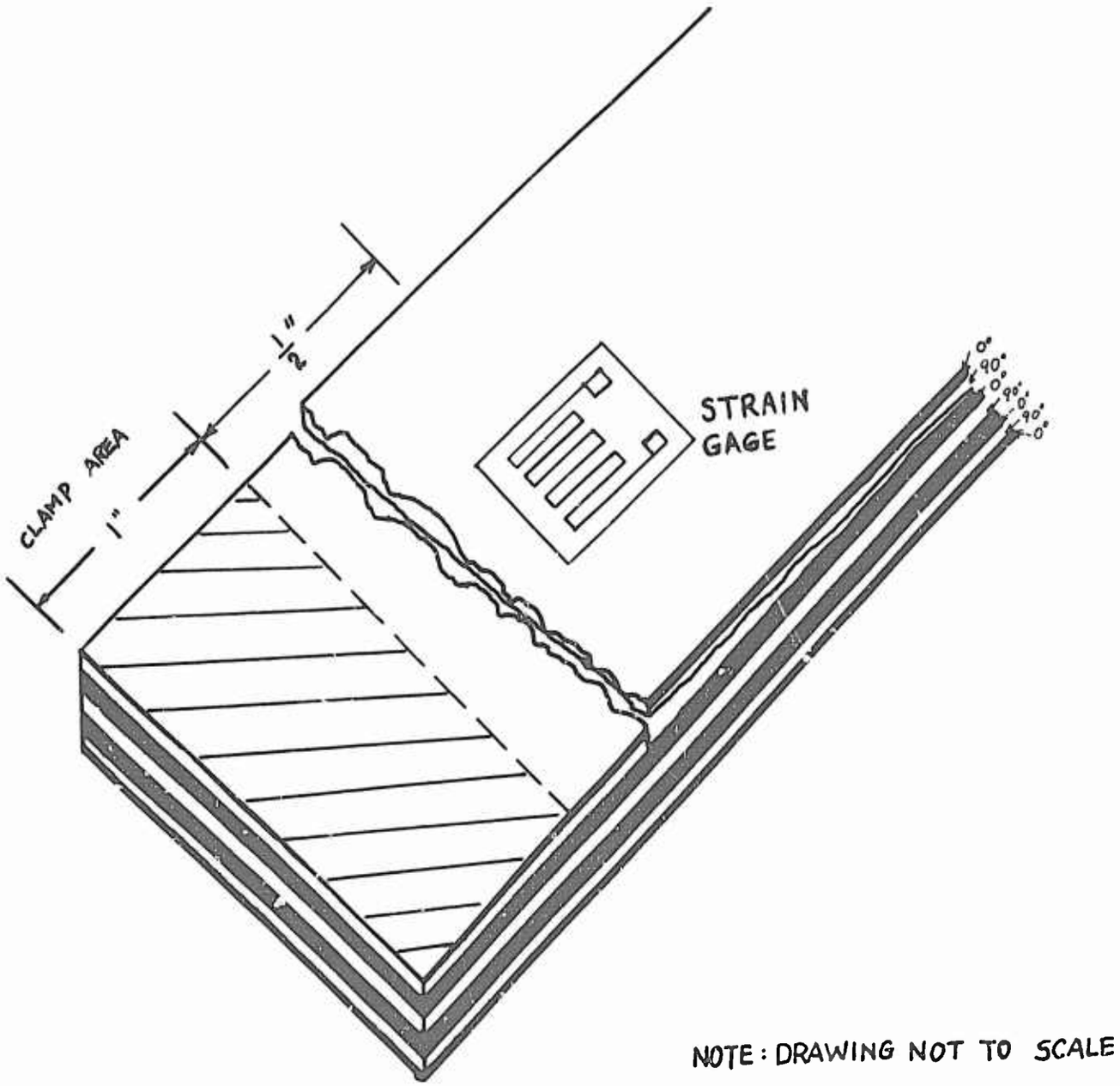

Figure 4. $[0/90]_{3S}$ Failure Pattern

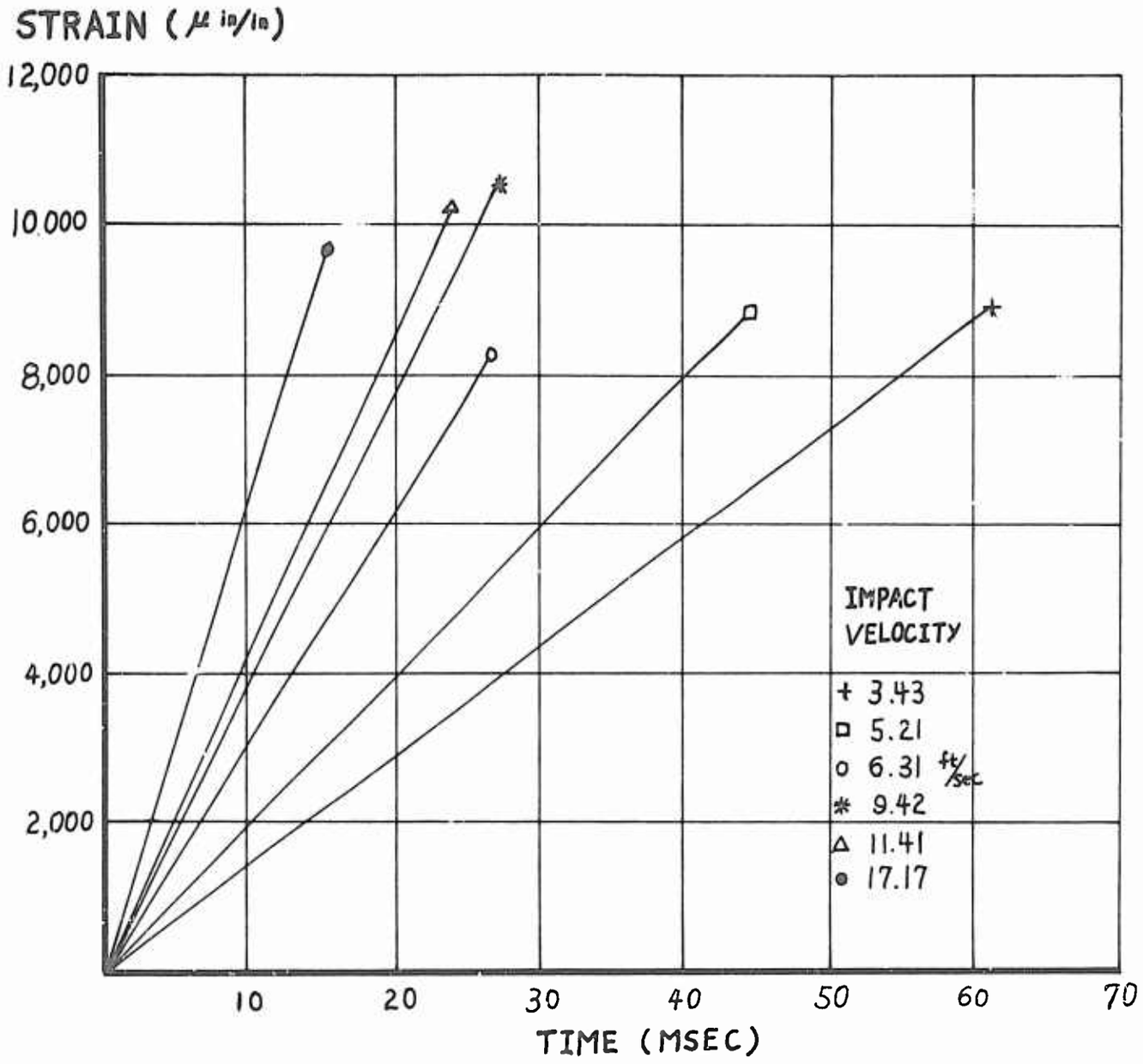

Figure 5. Strain-Time, $[0/90]_{3S}$

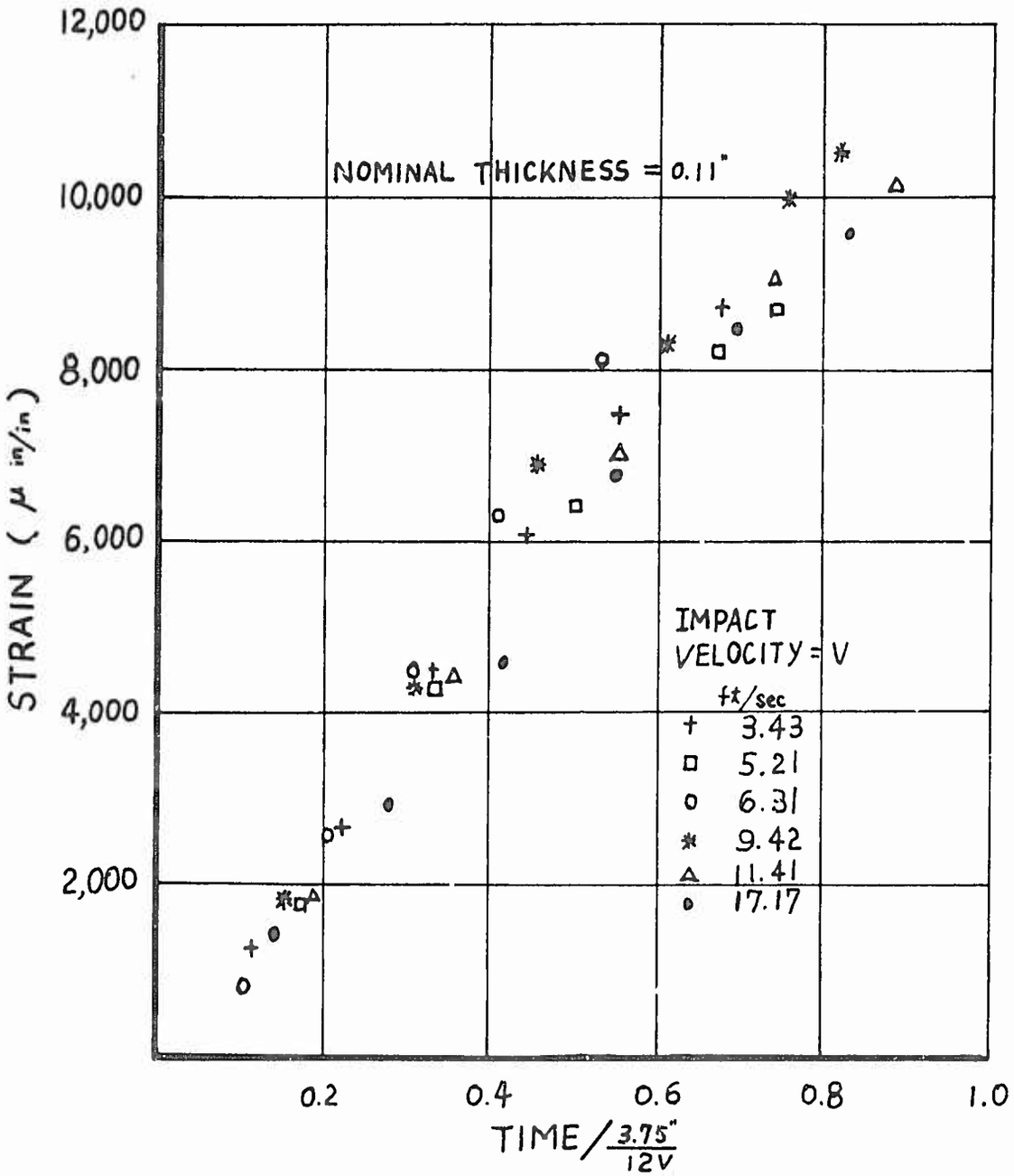

Figure 6. Strain-Dimensionless Time, $[0/90]_{3S}$

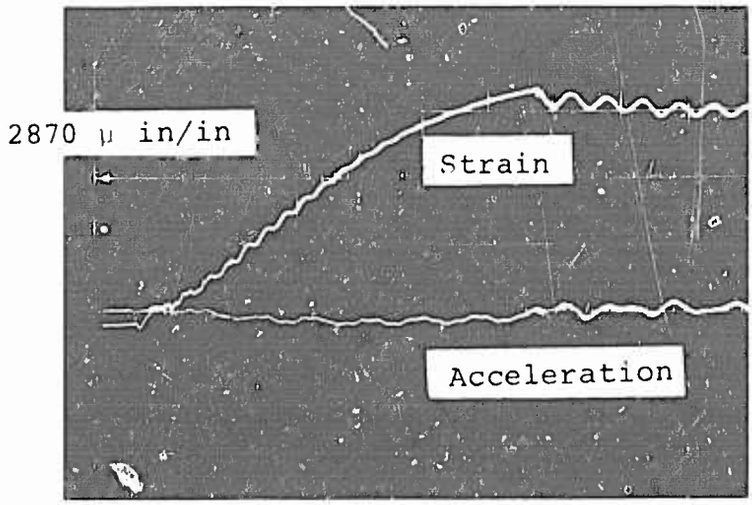

Time = 10 msec/div
Impact velocity = 5.5 ft/sec

Figure 7. Typical Oscilloscope Record, $[\pm 45]_{3S}$

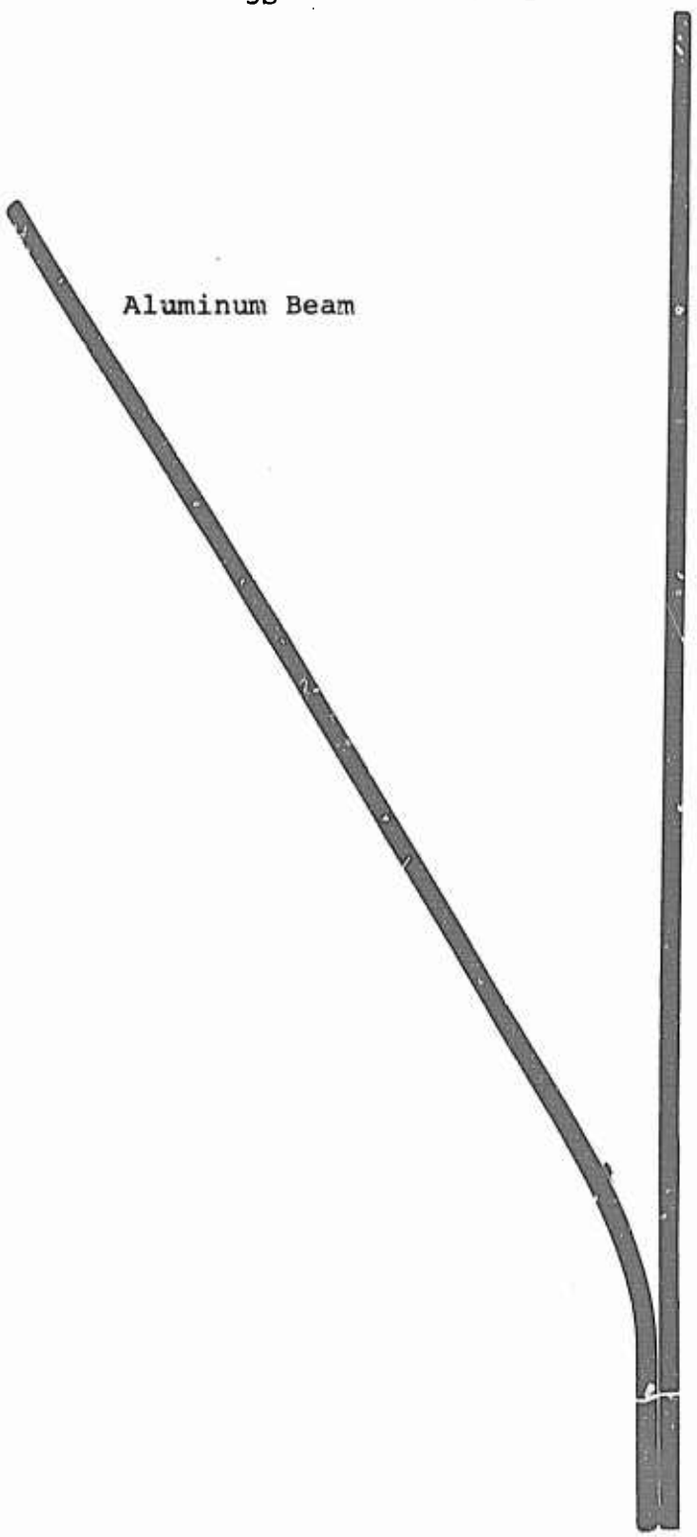

Figure 8. Aluminum Beam Compared with $[\pm 45]_{3S}$ Beam

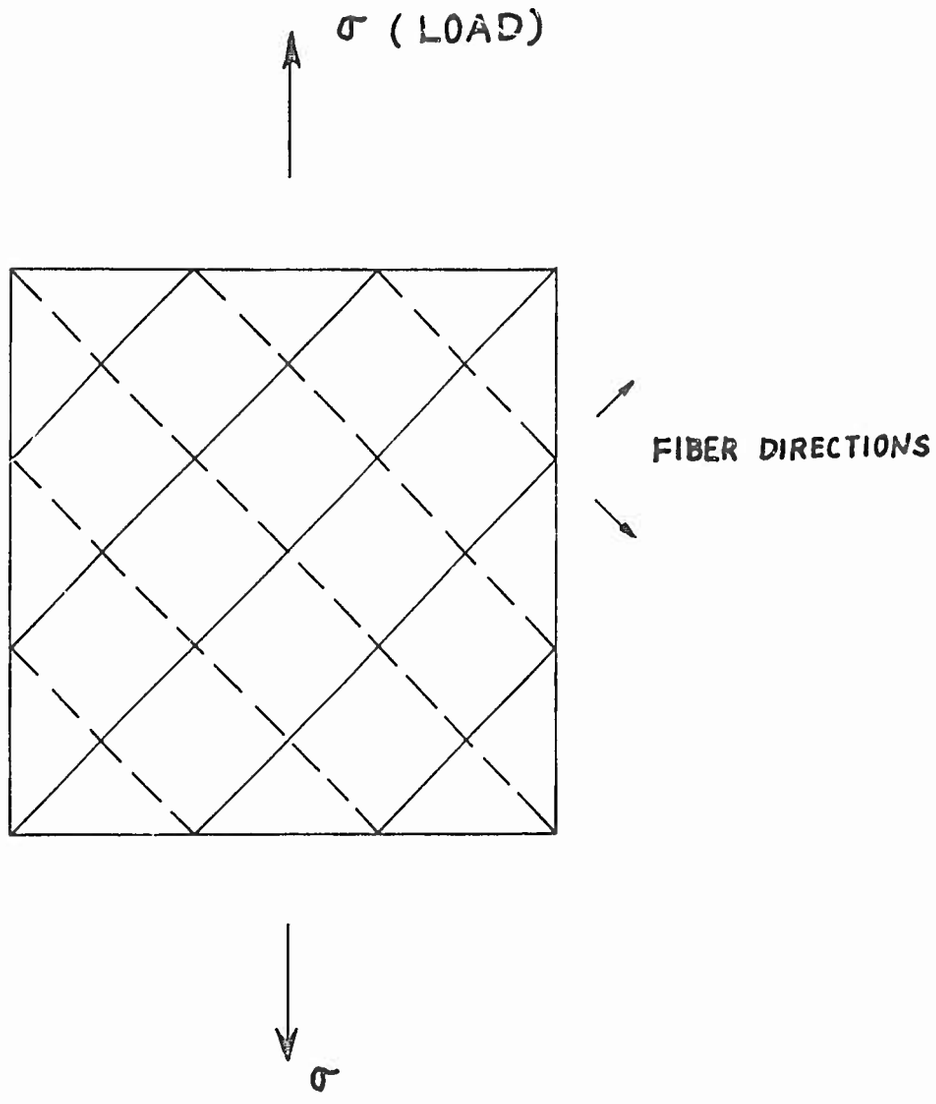

Figure 9. Free Body Diagram of $[\pm 45]_{3S}$ Beam Element

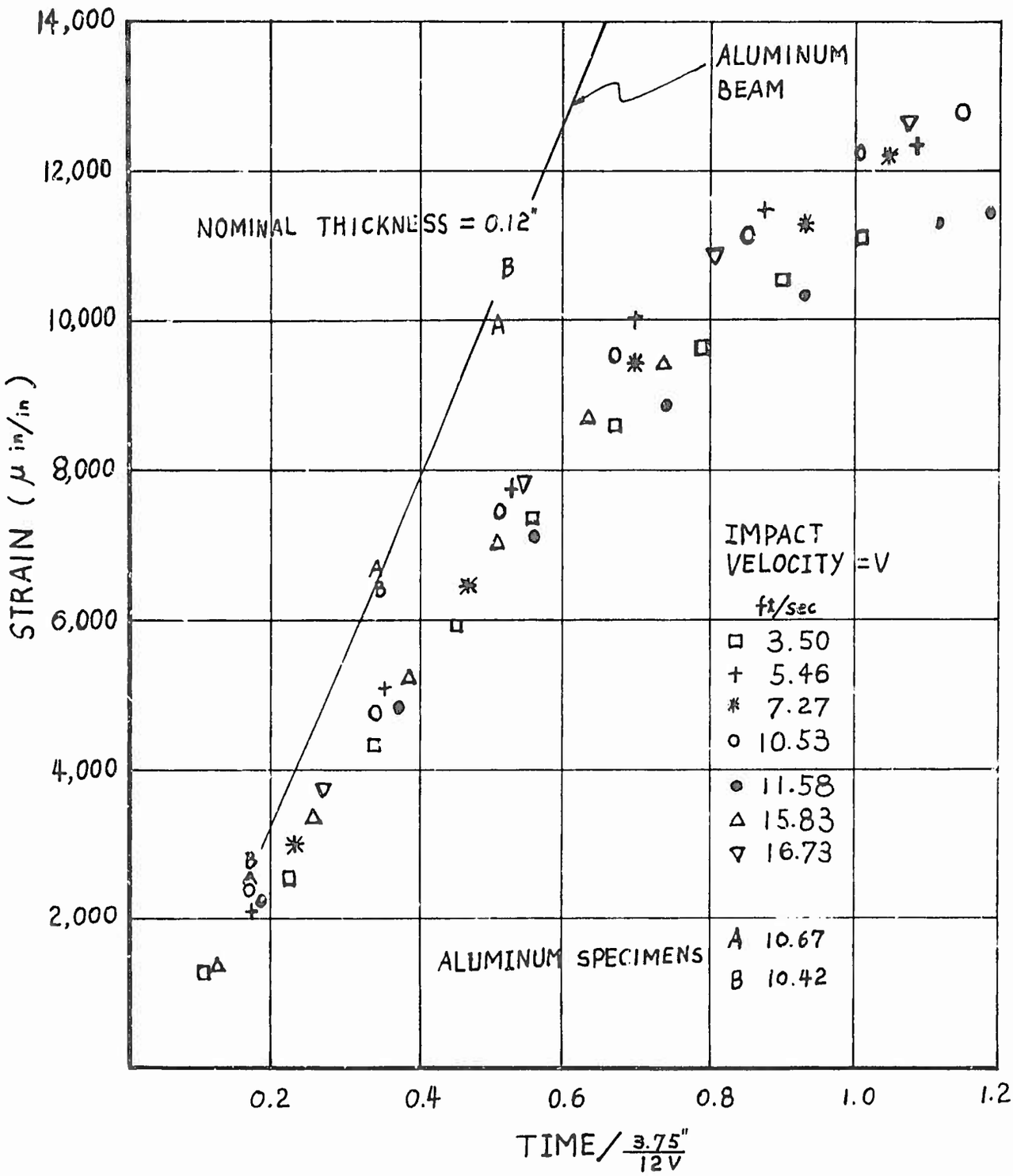

Figure 10. Strain-Dimensionless Time, $[\pm 45]_{3S}$

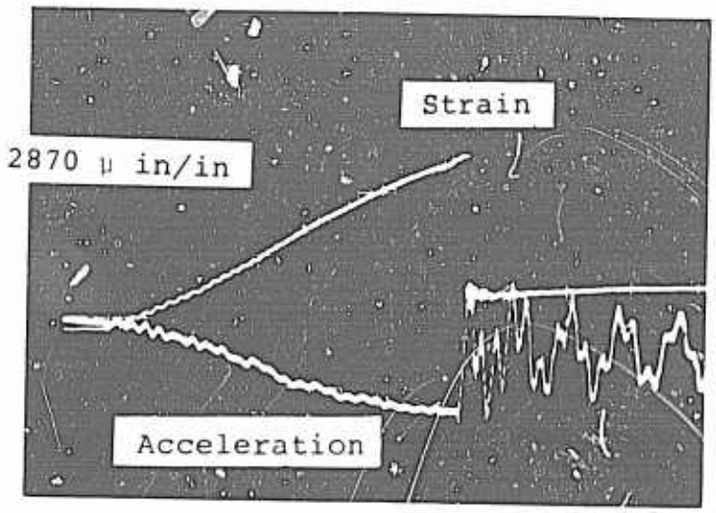

Time = 10 msec/div
Impact velocity = 3.2 ft/sec

Figure 11. Typical Oscilloscope Record, $[0/\pm 45/90/\pm 45/0]_S$

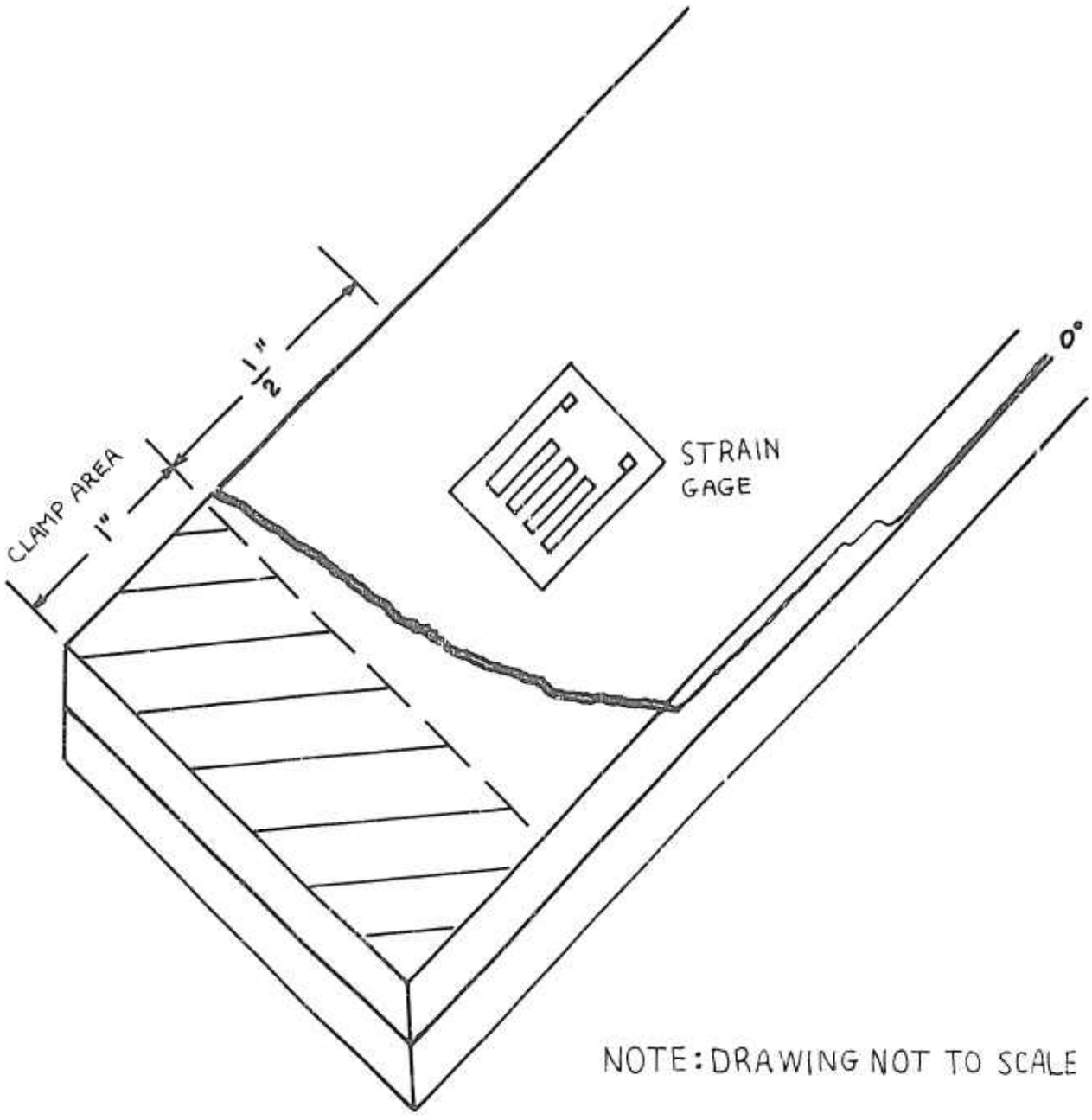

Figure 12. $[0/\pm 45/90/\mp 45/0]_S$ Failure Pattern

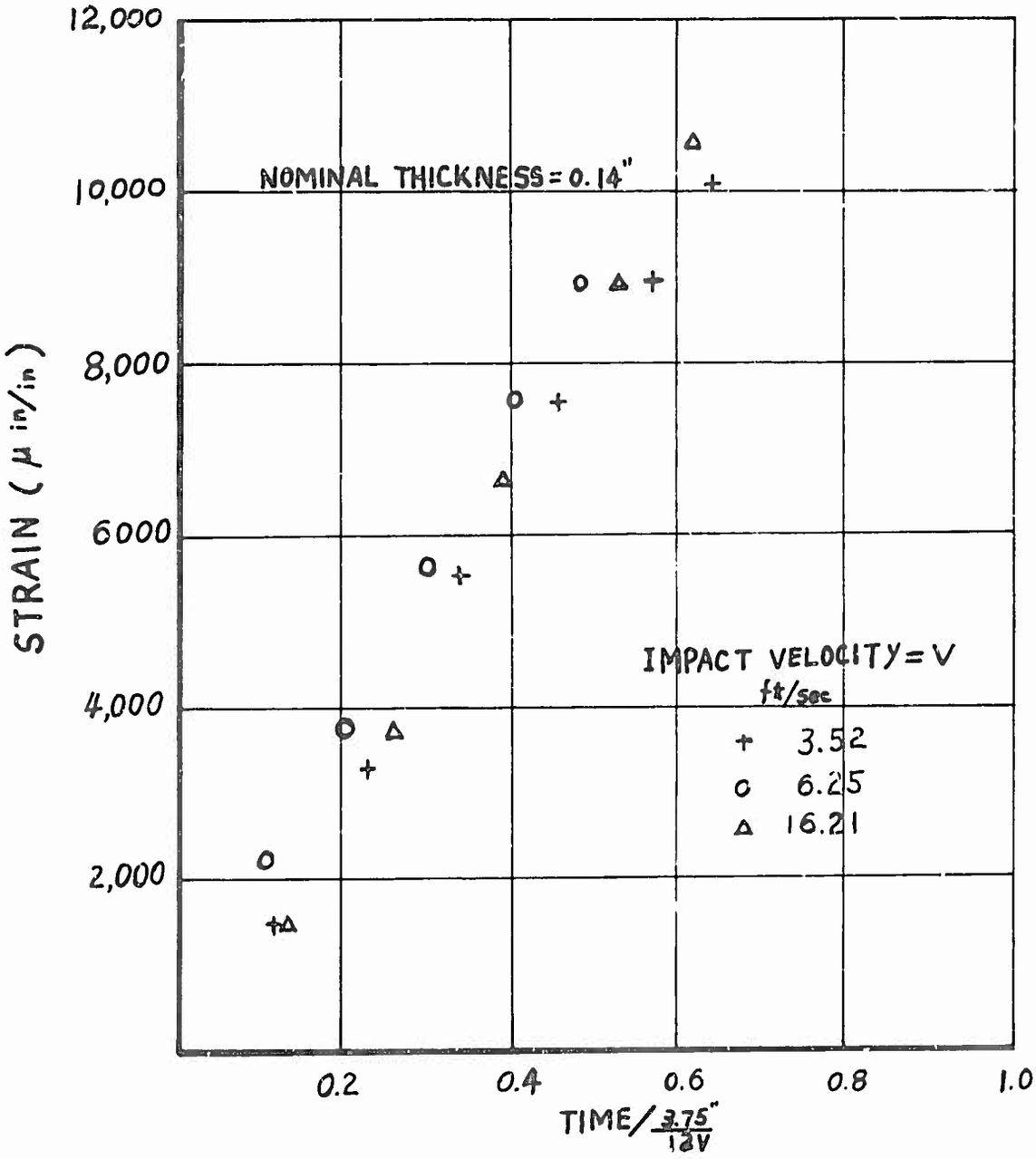

Figure 13. Strain-Dimensionless Time, $[0/\pm 45/90/\mp 45/0]_S$

REFERENCES

1. "Dynamics of Composite Materials," 1972 Joint National and Western Applied Mechanics Conference, edited by E. H. Lee, ASME Publication.

2. Achenbach, J. D., Herrman, J. H. and Ziegler, F., "Tensile Failure of Interface Bonds in a Composite Body Subjected to Compressive Loads," AIAA Journal, 6, October, 1968, p. 2040.

3. de Rosset, W. S., "Dynamic Fracture of Boron-Epoxy Composite," B.R.L. Memorandum Report no. 2319, August 1973. (AD #914015L)

4. de Rosset, W. S., "Response of Boron-Epoxy Composite to Impact Loading," B.R.L. Memorandum Report no. 2394, June 1974.

5. Armenakas, A. E., and Sciammarella, C. A., "Experimental Investigation of the Failure Mechanisms of Fiber Reinforced Composites Subjected to Uniaxial Tension," Technical Report AFML-TR-71-179, Air Force Materials Laboratory, August 1971.

6. Armenakas, A. E., and Sciammarella, C. A., "Response of Glass Fiber Reinforced Epoxy Specimens to High Rates of Tensile Loading," Technical Report AFML-TR-72-124, Air Force Materials Laboratory, January 1973.

7. Lifshitz, J. M., "Dynamic Moduli and Strength Properties of Some Fibrous Composite Materials," MED Report No. 33, Dept. of Materials Engineering, Technion-Israel Institute of Technology, Haifa, Israel, June 1971.

8. Schultz, A. B., and Tsai, S. W., "Dynamic Moduli and Damping Ratio in Fiber-Reinforced Composites," Journal of Composite Materials, Vol. 2, No. 3, July 1968, p. 368.

9. Sih, G. C., and Chen, E. P., "Fracture Analysis of Unidirectional Composites," Journal of Composite Material, Vol. 7, April 1973, p. 230.

10. Konish, H. J., Jr., Swedlow, J. L., and Cruse, T. A., "Experimental Investigation of Fracture in an Advanced Fiber Composite," Journal of Composite Materials, Vol. 15, January 1972, p. 114.

11. Waddoups, M. E., Eisenmann, J. R., and Kaminski, B. E., "Macroscopic Fracture Mechanics of Advanced Composite Materials," Journal of Composite Materials, Vol. 55, October 1971, p. 446.

12. Grimes, G. C., Francis, P. H., Commerford, G. E., and Wolfe, G. K., "An Experimental Investigation of the Stress Levels at which Significant Damage Occurs in Graphite Fiber Plastic Composites," Technical Report AFML-TR-72-40, Air Force Materials Laboratory, May 1972.

13. Grimes, G. C., Francis, P. H., Commerford, G. E., and Wolfe, G. K., "A Study of the Stress-Strain Behavior of Graphite Fiber Composites to Assess the Stress Levels at which Significant Damage Occurs," Technical Report AFML-TR-73-311, Air Force Materials Laboratory, January 1974.

14. Grimes, G. C., "Analysis of Discontinuities, Edge Effect and Joints," Treatise on Composite Materials, edited by Broutman and Krock, Academic Press, 1974.

15. Whitney, J. M., Grimes, G. C., and Francis, P. H., "Effect of End Attachment on the Strength of Fiber-Reinforced Composite Cylinders," Experimental Mechanics, Vol. 13, No. 5, May 1973, p. 185.

16. Yew, C. H., and Clark, L. G., "On Deformation of Laminated Shells," Journal of Applied Mechanics, March 1967, p. 227.